Combustion and Flame 188 (2018) 388–398

Contents lists available at ScienceDirect

Combustion and Flame

journal homepage: www.elsevier.com/locate/combustflame

An experimental study of horizontal flame spread over PMMA surface in still air

Oleg Korobeinichev[a,*], Munko Gonchikzhapov[a,b], Alexander Tereshchenko[a], Ilya Gerasimov[a], Andrey Shmakov[a,b], Alexander Paletsky[a], Alexander Karpov[c]

[a] Institute of Chemical Kinetics and Combustion, Novosibirsk 630090, Russia
[b] Novosibirsk State University, Novosibirsk 630090, Russia
[c] Institute of Mechanics, Izhevsk 426067, Russia

ARTICLE INFO

Article history:
Received 25 April 2017
Revised 26 June 2017
Accepted 5 October 2017

Keywords:
Horizontal flame spread
PMMA combustion
Flame structure
Microthermocouple
Probing mass spectrometry
Heat flux

ABSTRACT

The paper presents a comprehensive experimental study of flame spread over the surface of horizontally placed slabs of four types of PMMA specimens in still air. Temperature distributions in the gas phase near the solid fuel surface and in the condensed phase were measured using microthermocouples. Spatial variation of the species concentration in the gas-phase flame near the solid fuel surface was measured using probing mass spectrometry. Also flame spread rate over the polymer surface was measured. The experiments revealed differences in the combustion character of the specimens investigated. At the flame spread over surface of two (out of the four) specimens boiling and formation of large bubbles were discovered. The main flame components including MMA, O_2, CO_2, H_2O, N_2, C_2H_4 (ethylene), C_3H_6 (propylene) have been first identified, and their concentration profiles at different distances from the flame front have been measured. The data on the chemical flame structure have been shown to be in good agreement with the data on its thermal flame structure. The size of the "dark zone" of the flame, in which the temperature near the polymer surface is minimal, correlates well with the size of the oxygen-free zone, which is adjacent to the burning surface. Conductive heat feedback from the flames to the condensed fuel surface was estimated on the basis of the experimental results. The conductive heat flux averaged over the burning surface was estimated to be approximately 13.2 kW/m^2. It has been established that it is maximal in the flame front and decreases as the specimen burns out. The data obtained may be used for developing and validating a numerical model of flame spread over PMMA surface.

© 2017 The Combustion Institute. Published by Elsevier Inc. All rights reserved.

1. Introduction

Polymer materials are widely used in all areas—in the construction industry, in transport, in electro-technical industry and in people's households. As the number of fires has been growing recently, predicting the behavior of these materials in fire and reduction of polymers' flammability are becoming increasingly more important. Developing a model for combustion of polymer materials is thus becoming an important issue. Flame spread over the polymer surface during fire is one of the key processes resulting in initiation, spread and grow of fires. In the advanced flame-spread models, the heat flux from the flame to the virgin fuel is the key parameter that determines the flame spread rate. Although chemical reactions are the source of heat, insufficient attention has been paid to the study of their role in combustion of polymers and to development of their combustion models. This study is meant to eliminate this gap. It is devoted to further investigation of both thermal and chemical structure of flame spreading over polymer.

2. Literature review

A large number of studies [1–31] involve the study of the mechanism for the flame spread over polymer surface. In these papers, the mechanisms are studied for spread of laminar flames over flat surfaces of mostly polymethyl methacrylate (PMMA). The mechanism of the flame spread and simplified models depend on the thickness of the polymer specimens (slabs or cylinders) over which the flame spreads. Traditionally these specimens are divided into thermally thin, in which the temperature distribution across its thickness is an essentially uniform, and thermally thick, in which this distribution is not uniform. The mechanism for the flame spread depends on the angle of slope to the horizon of the polymer surface over which the flame spreads, the velocity and direction of the gas flow in relation to the vector of the flame spread,

* Corresponding author.
E-mail address: korobein@kinetics.nsc.ru (O. Korobeinichev).

https://doi.org/10.1016/j.combustflame.2017.10.008
0010-2180/© 2017 The Combustion Institute. Published by Elsevier Inc. All rights reserved.

and gravitation. Most papers discuss downward and upward flame spread over the fuel slab. Measurements have been performed of the flame spread rate, of the temperature fields in both gas and condensed phase and velocity fields in the gas phase. The methods used include thermocouple probing, photographing, measuring flame luminescence and radiation, sampling gaseous combustion products from the flame, followed by their analysis by gas chromatography. Noteworthy that the physical and chemical characteristics of the investigated polymer (PMMA) and information regarding the polymer manufacturers are provided in not all the papers describing the experimental studies. Thus, comparison between various experimental data is not always available.

Simplified theoretical models have been developed for the flame spread. They include the mechanisms of heat transfer to the polymer surface in the boundary layer, which is situated downstream the flame front near the flame attachment zone. Applicability of these physical models to other materials depends on the thermal and chemical kinetic properties of these materials. A review of the theoretical models of opposed-flow flame spread developed before 1992 has been published earlier [9]. There are few papers considering numerical modeling of flame spread over polymer surface [7,12–17], in which the model includes energy equations with chemical reactions for the gas-phase and solid-fuel equations based on pyrolysis kinetics. There are even less papers in which the results of numerical modeling are compared with experimental data. Horizontal flame spread over a polymer surface is a slow process compared to other flame spread configurations and is an important area of study due to its simplicity and suitability for theoretical analysis. In [1,5,20], the experimental results of the horizontal flame spread over thermally thick slabs of PMMA of various thickness (1.6–25 mm) are discussed. Ray et al. [5] investigated the mechanisms of heat transfer in horizontal flame spread over thermally thick PMMA slabs in still atmosphere. Using chromel/alumel thermocouples 0.025 mm in diameter, authors [5] measured the temperature fields on the polymer surface and inside the polymer, while the Pt/Pt13%Rh thermocouples 0.025 mm in diameter were used to measure the temperature fields upstream from the flame front for horizontal flame spread over PMMA slabs 2.54 cm thick. The authors revealed that, unlike in the case of vertically downward flame spread, radiation heat transfer from the flame to the fuel can play a significant role in the heat transfer process for the horizontal mode of flame spread. They also measured the heat fluxes and the gas flow velocity fields upstream at different distances upstream from the flame front. Analysis of the data obtained indicates that there is a transition in the mechanisms of heat transfer as the fire grows. While in the early stages of the fire, heat conduction through the solid is dominant, radiation from the flame becomes of increased importance as the size of the fire increases.

In [18] the rate of flame spread over the surface of thick PMMA (12.7 mm thick) was measured as a function of the velocity and oxygen content of a gas flow opposing the direction of flame spread. At low flow velocities, the flame spread rate was shown to be practically independent upon the gas flow velocity. The experimental results agreed with predictions of the simplified flame spread model, which contained two components: the gas-phase kinetic and the heat transfer from the flame to the fuel. Jiang et al. [27] experimentally and theoretically investigated the influence of the slab width on horizontal flame spread over slabs of extruded polystyrene and expanded polystyrene foams, used for heat insulation of the external walls of buildings. Polymer slabs were placed on a thermal insulation board, which was mounted on an electronic balance, providing determination of the mass loss rate. The flame spread rate depended on the slab width. Minimum values of the flame spread rate were found for extruded polystyrene foam.

In Ref. [27], based on the experiments conducted, a simplified model of horizontal flame spread over various widths of polymer foams was developed. In [28], the model was improved by performing similar experiments with a simpler fuel, namely, PMMA. Slabs of extruded PMMA from 2 to 6 mm thick and 50–100 mm wide were used. The specimens were manufactured by Nanchang Inter Industrial Co. Ltd. The flame spread rates, convective and radiation heat fluxes from the flame to fuel were measured for various widths and thicknesses of the specimens. Comparison of the data [28] on the flame spread rate over the surface of the PMMA specimens with those from papers [1,5,20] for similar thickness and width revealed 4–5 times divergence. To reveal the causes of such disagreement analysis and further experiments are required. It may be connected with the differences in the physical and chemical structure and properties of the polymer specimens and, therefore, in kinetic parameters of pyrolysis of the indicated specimens and their influence on the flame spread rate. Current studies and the models for polymer combustion consider the chemical aspect of the combustion process insufficiently. Actually the chemical structure of the flame spreading over polymer materials has not been investigated earlier. Experimental data on the concentration profiles of species in a polymer flame spreading over the polymer have not been reported. These data are of great demand for developing of a detailed model for flame spread over the polymer, considering the kinetics of polymer pyrolysis and the pyrolysis products, as well as the gas-phase reactions of the products combustion.

The goal of present research consists in continuation of the experimental study of the thermal and chemical structure of flame during its horizontal spread over PMMA slabs in still atmosphere. The results obtained may be used for developing and validating a numerical model for this process.

3. Experimental

Four types of PMMA slabs have been investigated. Their physico-chemical properties and the manufacturers are shown in Table 1. The heat of polymer gasification Q_g is equal to the sum of the heat required to heat the specimen from room temperature to pyrolysis temperature and the pyrolysis heat H_p. We determined the heat of polymer gasification as described in [29] using the DSC method.

Polymer slabs 50 and 100 mm wide, 5 mm thick and 200 mm long were studied. The slabs were inserted into a thin metal frame to prevent flame spread over the side surfaces and were placed horizontally on an incombustible heat insulating plate 10 mm thick (see Appendix A), which was positioned on an electronic balance. The thermal conductivity and specific heat of the insulation board were, respectively, 0.15 W/m K and 950 J/(kg m K). To determine spread rate of the flame over the slab, horizontal marks were made on the specimen surface with a 5 mm step. The slabs were ignited from its edge by the flame of a propane-butane burner. During ignition, the upper surface of the slab was protected from flame with an incombustible heat insulating plate, which was removed after the slab was ignited. The rate of the flame spread over the horizontal polymer surface and the mass loss of the polymer slab were determined from the video of the experiment. To measure the temperature profiles in the fuel, three thermocouples made from Pt and Pt+10%Rh wire 50 μm in diameter were used. Thermocouples 1 and 3 were mounted on the upper surface of the slab at a distance of 120 and 130 mm from the frontal edge of the slab. Thermocouple 2 was fixated on the lower surface of the slab at a distance of 120 mm from the frontal edge of the slab. The thermocouples were installed in a groove (0.2–0.3 mm deep) made on the slab surface. The thermocouple and the groove were

Table 1
The physico-chemical properties and the manufacturer of the specimens studied.

Specimen	Manufacturer	Method of producing	MW (g/mol)	ρ_s (g/cm^3)	H_p (J/g)	Q_g (J/g)
PMMA 1	Unknown	CAST	7.03×10^5	1.16	810 ± 80	1880 ± 180
PMMA 2	Evonik Rohm GmbH, Germany	Extruded	1.14×10^5	1.16	995 ± 100	1980 ± 200
PMMA 3	Marga Cipta brand, India	CAST	13.8×10^5	1.16	1020 ± 60	2010 ± 110
PMMA 4	*	Extruded	0.71×10^5	1.14	1100 ± 100	2085 ± 215

* Specimen 4 slabs were prepared by hot pressing of pellets PMMA (manufactured by CM-211, Chi-Mei Company, Taiwan) at 190 °C under the pressure of 10 atm during 1 min. H_p—effective heat of pyrolysis, Q_g—heat of gasification, MW—molecular weight, ρ_s—specific density.

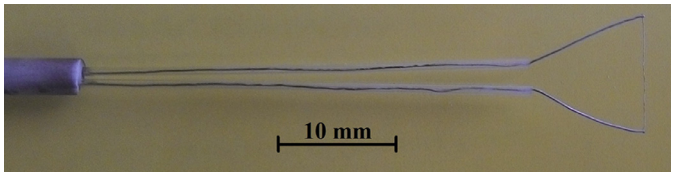

Fig. 1. A photo of thermocouple 4.

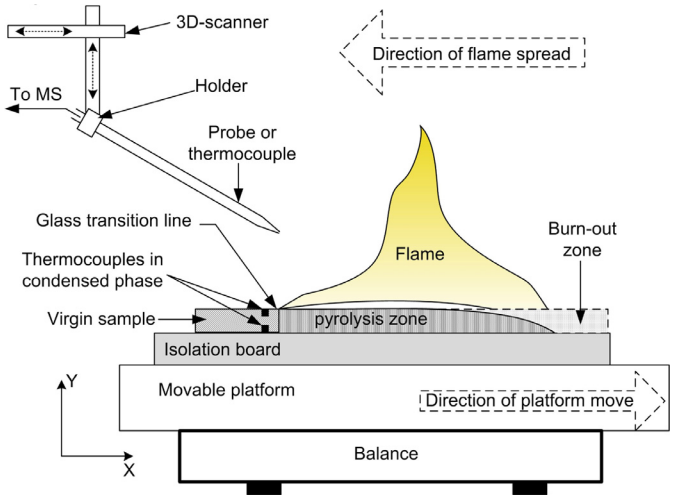

Fig. 2. The experimental apparatus for studying horizontal flame spread over solid fuel and for measuring the temperature and species concentration profiles.

covered with a layer of glue, which was a 50% solution of PMMA in dichloroethane.

Thermocouple 4 made of Pt and Pt+10%Rh wire 50 µm in diameter was used to measure the flame temperature (Fig. 1). The diameter of its junction was 80 µm, and the thermocouple shoulders made from 50 µm wire were 5.5 mm long. The shoulders of thermocouple 4 were welded to the Pt and Pt+10%Rh wires 0.2 mm in diameter, which were placed into quartz capillaries 0.7 mm in diameter inserted into a ceramic tube 3 mm in diameter and 70 mm long. The outstanding length of the capillaries was 40 mm. Thermocouple 4 was coated with SiO_2 layer 10 µm thick. It was fixated on a 3D-scanning device with three stepper motors, allowing the thermocouple to be moved in three coordinates in accordance with the program set. The correction for radiation heat loss for the thermocouple was estimated using the formula provided by Kaskan [30]. For maximum measured temperature $T_c = 1940$ K, this correction gives 190 K. The temperature measurements were performed as follows. Thermocouple 4 was placed before the flame front at the height of 30 mm from the specimen surface and was periodically moved at the velocity of 2 mm/s until it reached the slab surface. The thermocouple's contact with the slab surface was controlled with the electronic balance. The thermocouple's design allowed its contact with the slab surface without deforming the thermocouple's shoulders. Resolution along the *X*-axis depended on the spread rate of the flame front. So, the distance between the passages of thermocouple varied from 0.7 to 1.7 mm for different samples. As the flame front moved over the specimen surface, the range of downward movement of the thermocouple was increased gradually with a step of 1 mm. That was required for the thermocouple to reach the burning surface of the polymer as close as possible, the position of which was shifted downwards as the slab was burnt-out.

The temperature gradient in the gas phase near the slab surface was determined from the experimentally measured temperature profiles by calculating the maximum derivative of the temperature by the height over the polymer surface. The temperature gradient in the beginning of the flame zone (0–12 mm from the flame front) was found at the height of 0–2 mm from the initial polymer surface. For the distances from 12 to 30 mm from the flame front, the range of the heights from 0 to 1 mm from the burning surface was required for finding the temperature gradient. At the distance of over 30 mm from the flame front, the temperatures were found in the range of the heights from −1 to 0 mm from the initial polymer surface due to specimen burn-out. As the temperature profile was measured along coordinate *Y*, the measurement interval during movement of the thermocouple along the *X* axis was 0.5–1 mm, at the distance of 12 mm from the flame front and 1.5 mm at the distance exceeding 12 mm from the flame front.

A similar technique was applied by Singh and Gollner to measure conductive and radiation heat fluxes over burning PMMA specimens [31,32].

The schematic of the setup is shown in Fig. 2. Shown in Fig. 3 are the photos of the experiment on measurement the flame temperature (right) and of microprobe sampling from PMMA flame (left).

In measuring the temperature profiles, the signals from the thermocouples were recorded with a 14-bit AD converter E14-140-M. Temperatures were taken 3 times for the same experimental setup to ensure repeatability. All the types of heat fluxes (heat conduction, convection and radiation) were measured only in the steady combustion mode, i.e. the mass loss rate, the pyrolysis length and the flame spread rate were constant.

Before the flame reached the back edge of the specimen, it was extinguished to measure the contour of the pyrolysis zone, showing dependence of the thickness of the unburnt part of the specimen versus the distance from the flame front. For this purpose, the extinguished specimens were cut in the middle lengthwise, as slight distortion of the flame front was observed on the border of contact of the slab with the metal frame, and were photographed. The extinguished surface of the polymer was also photographed, and the length of the pyrolysis zone L_p (the distance from the flame front to the line of complete burnout of the specimen) and its area were measured. In addition, the length of the pyrolysis zone for extinguished specimens was compared with video measurements of this length. The line of the beginning of the pyrolysis zone was considered as the flame front, which is clearly visible in the extinguished specimens as well as the line

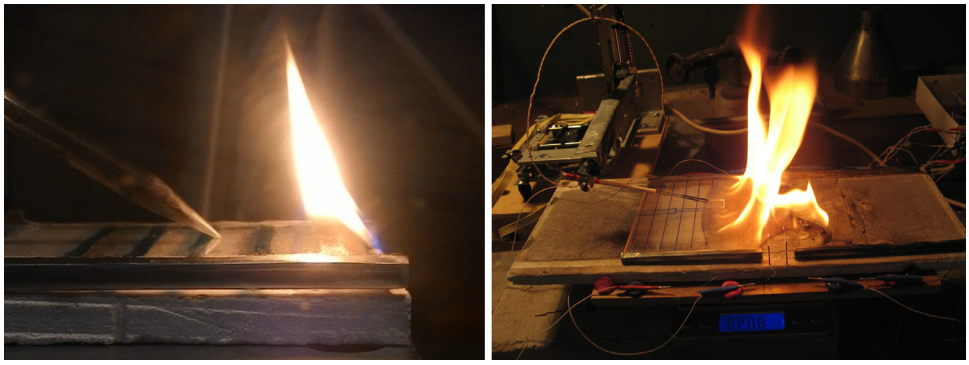

Fig. 3. Photos of the experiment on measurement the flame temperature (right) and of microprobe sampling (left) from PMMA flame.

of glass transition. According to [4] the temperature of the glass transition is 125 ± 10 °C.

The chemical structure of the flame was measured using a quartz microprobe with the orifice diameter of 60 µm. The internal angle of the probe's opening at the cone base was 20°. To prevent the clog of the probe orifice by the forming soot, an electric magnet was installed inside the probe, with a rod, at the end of which tungsten wire 20 µm in diameter was fixed. The rod moved toward the probe orifice in such a way so that the wire emerged to the length of about 1 mm and then returned to its previous position with frequency 3 Hz. A pulse generator was used to control the magnet.

The probe was also mounted on the 3D-scanning device, and gas samples were introduced into the ion source of Hiden HPR 60 mass-spectrometer as molecular flow and were analyzed. At the beginning, the probe was positioned at the height of 30 mm above the PMMA slab surface at the distance of 10 mm from the flame front. The probe was moved in the vertical direction at the velocity of 1 m/s until it touched the surface. After touching, the probe returned to the original position and was then moved horizontally to the distance of 5 mm toward the flame front. The procedure was repeated until the entire pyrolysis zone was covered. To increase the accuracy of measuring the species concentration profiles, spatial stabilization of the flame was carried out. For this purpose, the PMMA slab was mounted on a platform, which was moved in the horizontal direction with a stepper motor. The platform was moved in a direction opposite to that of the flame with the velocity equal to the rate of flame spread over the surface. The platform started to move after the flame spread rate reached a constant value. The interval for measuring the species concentrations along the coordinate Y was equal to approximately 0.35 mm, whereas that along the coordinate X was 5 mm.

It is to be mentioned that previously in [33] a special device was described designed to stabilize flame at its spread over the polymer surface. To suppress flame fluctuations caused by the perturbance of the ambient air, the experimental setup was enclosed with a net, with the mesh size 1×1 mm. The temperature and the species concentration profiles were measured in the plane crossing the middle of the specimen and perpendicular to its surface and to the flame spread front. This allowed determining two-dimensional temperature and species concentrations distributions in the PMMA flame (Fig. 3).

For all the major species discovered in the PMMA flame (methyl methacrylate (MMA), C_2H_4, C_3H_6, O_2, CO_2, H_2O), calibration tests were conducted, and calibration coefficients were obtained. The procedures of determining the mole fractions of the species has been described earlier [34]. The concentration profiles of the species were averaged by the distance from the burning surface to the flame. The averaging was carried out in the Origin software by the adjacent-averaging method. The major error of measuring species concentrations is related to reproducibility of measurements. According to averaging of the measurement data obtained in three tests, the relative measurement error for N_2, O_2, CO_2 was not more than 10%, for MMA it was 15–20%, for H_2O, 20%, and for C_2H_4 and C_3H_6, 20%. The time of measuring species in the PMMA flame was for N_2, O_2, CO_2, C_2H_4, C_3H_6 10 ms and for MMA and H_2O, 50 ms.

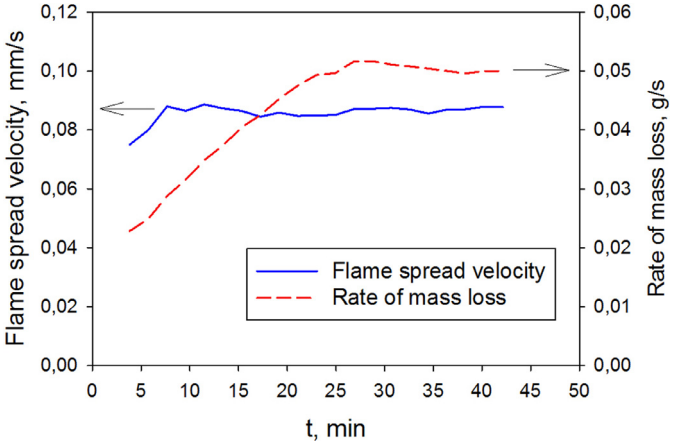

Fig. 4. The time dependences of the flame spread rate u_f over the surface of specimen 3 and the specimens' mass loss rate.

In order to determine the temperature gradient near the flame front more precisely we conducted experiments using a flame stabilization system. The temperature profile near the flame front (from −5 mm to 10 mm) was measured with the interval of 1 mm in the horizontal direction and with the interval of 0.005 mm in the vertical direction. The thermocouple was moved to the polymer surface with the velocity of 0.5 mm/s.

4. Results and discussion

4.1. The flame spread rate over the surface of specimens of different types of PMMA and the specimens' mass loss rate

In Fig. 4 the time dependences of the flame spread rate u_f over the surface of specimen 3 and the specimens' mass loss rate are shown. Analysis of the data shown in Fig. 4 has indicated the stationary mode to appear at the 7th minute for the flame spread rate, and for the mass loss rate it starts 24 min after the beginning of the specimen's burning, when combustion is stable.

Table 2 shows the results of measuring the flame spread rate, the mass loss rate U_{mas}, the length of the pyrolysis zone L and the mean mass pyrolysis rate W, determined for different PMMA slabs with varying width L_w and thickness h. The mean mass pyrolysis

Table 2
The flame spread rate and the mass loss rate, the length of the pyrolysis zone and the mean mass pyrolysis rate, measured for the studied PMMA specimens with different width and thickness.

Specimen	L_w (mm)	h (mm)	u_f (mm/s)	U_{mas} (g/s)	L (cm)	$\dot{m}$ (g/s cm^2)
1	100	5	0.1	0.04	6.5	7.5×10^{-4}
1	50	5	0.09	0.027	6.1	10^{-3}
1	100	1.7	0.11	0.03	2.5	1.7×10^{-3}
2	100	5	0.07	0.045	5.2	0.9×10^{-3}
3	100	4.65	0.09	0.05	5.2	10^{-3}
4	50	4	0.025	0.0074	1.4	10^{-3}
4	100	4	0.027	0.014	1.9	7.3×10^{-4}

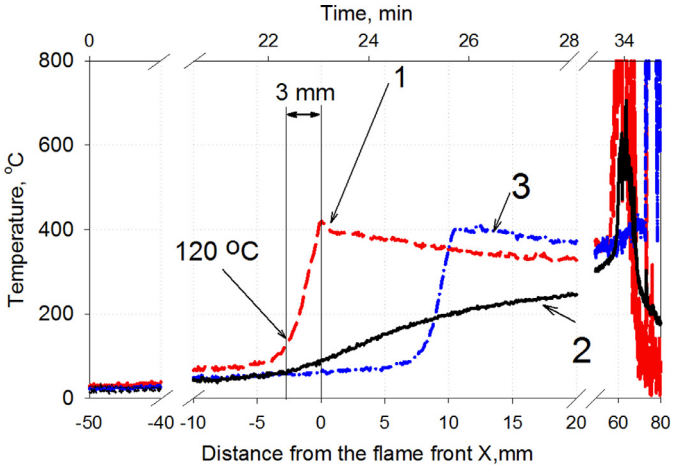

Fig. 5. The time and the distance from the flame front dependences of the temperature of the upper surface (curves 1 and 3) and the lower surface (curve 2) of the slab of specimen 3.

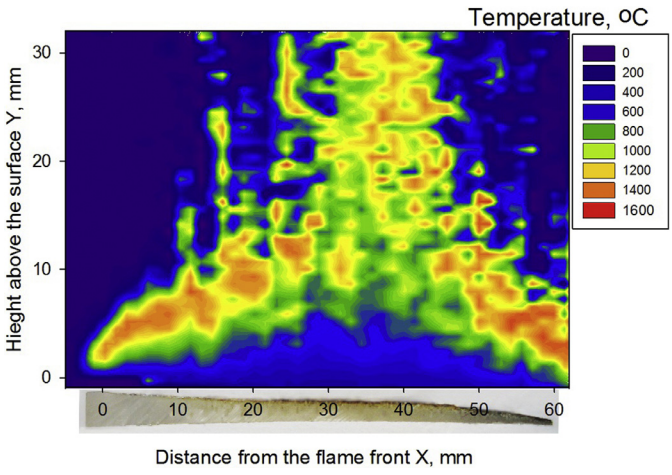

Fig. 6. The temperature variation in the gas phase over the burning surface of the specimen 3.

rate, equal to the mass loss rate divided by the area of the pyrolysis zone, was calculated by the formula $\dot{m} = U_{mas} / L_w \cdot L$. The values obtained were measured in the mode where stable combustion was achieved. Variance of the flame spread rate data u_f was 10%.

It can be seen that change in the width of specimen 1 from 50 to 100 mm did not result in the change of the spread rate. At the same time, the flame spread rate for specimens 1–3 is close to the results obtained in [1,5,20] for plexiglass specimens and is about 3 times less than that obtained in [28] for extruded PMMA manufactured by Nanchang Inter Industrial Co. Ltd. The flame spread rate for pressed PMMA was 4 times lower than for specimens 1–3 and was more than by an order of magnitude less than for the specimens studied in [28]. In fact, triple reduction in the thickness of specimen 1 produced no effect on the flame spread rate but resulted in 2.4 times reduction of the length of the pyrolysis zone and in the 1.7 times increase of the mean mass pyrolysis rate. It is noteworthy that the mean mass pyrolysis rate for all the specimens 4–5 mm thick was practically equal and constituted 7.3×10^{-4}–10^{-3} g/(s cm^2).

4.2. Temperature fields at horizontal flame spread over PMMA surface

Figure 5 shows time and the distance from the flame front dependences of the temperature of the upper surface (curves 1 and 3) and the lower surface (curve 2) of the slab of specimen 3 (measured by using three thermocouples). The distance between thermocouples 1 and 3 was 10 mm. Comparison of curves 1 and 3 confirms the conclusion regarding the stationary character of combustion during the temperature measurements in the flame. Thermocouple 2, which was at the same distance from the front edge of the slab as thermocouple 1, allowed heat penetration into the specimen in the direction perpendicular to the slab surface to be evaluated. It can be seen from Fig. 5 that the temperature of the PMMA burning surface first reaches its maximum near the flame front and then slowly goes down in the central flame zone as the specimen burns out. Figure 5 demonstrates that the investigated case of combustion of a 5-mm-thick PMMA slab is related to the half-way regime, which is intermediate between the thermally thick and thermally thin combustion modes.

When the thickness of the unburnt part of the fuel decreases considerably, the thermocouple junction becomes exposed to the gas phase. In Fig. 5, this moment corresponds to a dramatic rise of temperature from 400 °C to 1000–1200 °C. Figure 6 shows the temperature variation in the gas phase over the burning surface of the specimen 3; the temperature profiles are recorded at different distances X from the flame front; flame spreads from left to right. Hereinafter, the flame front corresponds to the beginning of the fuel pyrolysis zone. The distance between them is 3 mm. Axis Y corresponds to the vertical distance from the surface of the virgin fuel.

In the lower section of Fig. 6, there is a photograph of the cross-section of the extinguished specimen after the experiment, showing dependence of the thickness of the unburnt part of the specimen on the distance to the flame front. It can be seen that the height of the 'dark zone' over the polymer surface, in which the flame temperature does not exceed 1000 K, increases as the distance from the flame front increases, and the height of the reaction zone of the flame (the flame height) increases, too. The position of the flame leading edge coincides with the flame front edge. From the spatial distribution of temperature shown in Fig. 6, it can be seen that the flame temperature fluctuations intensify as the height over the fuel surface increases. The observed phenomenon is explained by intensification of turbulence of the gas flow due to convective rise of the hot combustion products. Figure 7 shows dependences of the flame temperature on the distance from the sur-

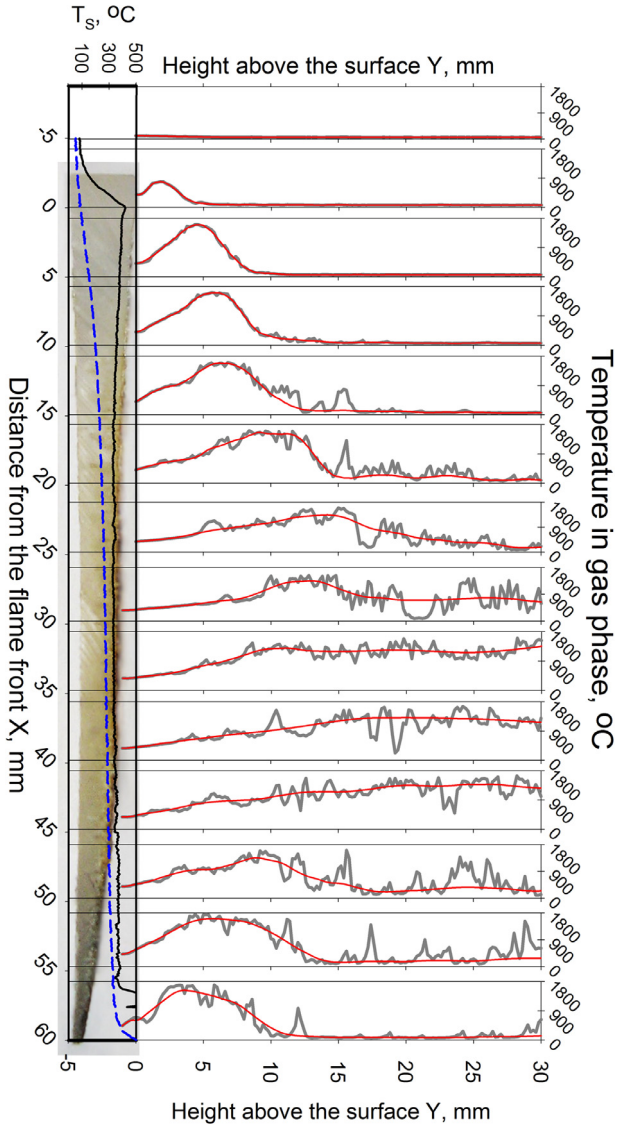

Fig. 7. Dependences of the flame temperature on the distance from the surface (Y) of virgin specimen 3 measured at different distances from the flame front (X) and smoothed temperature profiles (right). Dependences of the temperature of the upper surface (solid line), the lower surface (dotted line) of fuel and the thickness of the unburnt part of the specimen on X (left).

face (Y) of virgin specimen 3 measured at different distances from the flame front (X) (right). Besides, dependences of the temperature of the upper surface (solid line) and the lower surface (dotted line) of fuel and the thickness of the unburnt part of the specimen on the X-direction are shown in Fig. 7 (left).

Figure 7 demonstrates the temperature profiles to be rather smooth near the polymer burning surface, whereas, essential temperature fluctuations take place as the distance from the specimen surface increases. The cause of the fluctuations has been indicated above. In addition to the temperature profiles shown in Fig. 7, we have provided smoothed temperature profiles, without temperature fluctuations caused by turbulence, which may be used by the CFD modelers to perform a meaningful comparison with simulation data. The length of the pyrolysis zone was shown to be about 60 mm. As seen from the photograph of the flame of specimen 3 (Fig. 8), maximum flame height was about 120 mm.

Correction for radiative heat losses of the thermocouple was estimated to be approximately 60–70 °C for maximum temperatures. The data shown in Fig. 7 were used to calculate the dependence

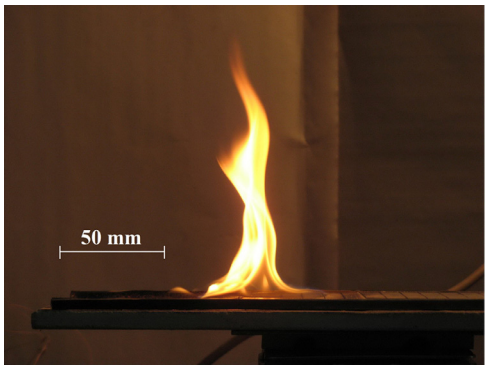

Fig. 8. A photo of the flame of specimen 3 (width 100 mm).

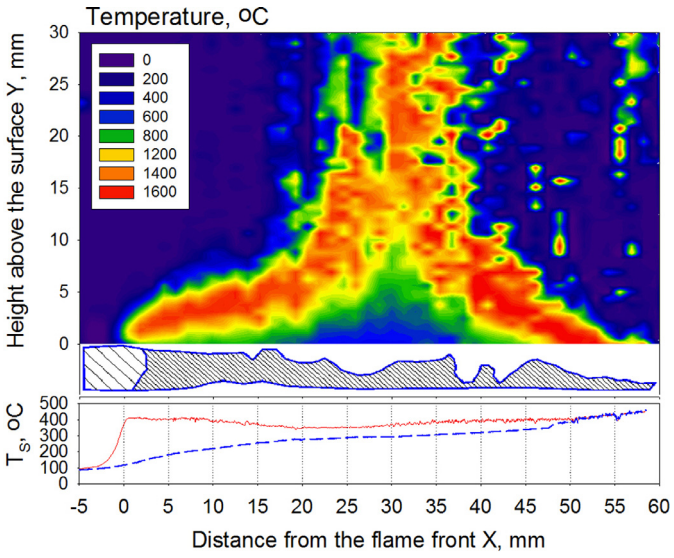

Fig. 9. The spatial distribution of temperature in the flame and in the condensed phase of the burning specimen PMMA 2. At the bottom of the figure there is the contour of the cross section of the extinguished specimen and dependences of the temperature of the upper surface (solid line) and the lower surface (dotted line) of fuel on X-direction.

of the temperature gradient near the burning surface on X. The error of evaluating the temperature gradients was about 15–20%. The data shown in Figs. 5–7 were first obtained for horizontal flame spread over the surface of a PMMA slab 5 mm thick. Previously there were only data [5] on the temperature fields in the gas and condensed phases before the flame front spreading horizontally over a PMMA slab 25 mm thick. It can be seen from Fig. 5 that the gas temperature at the distance of 10 mm before the flame front is higher than the ambient temperature (25 °C), which confirms the importance of the contribution of the flame radiation to the heat flux on the polymer surface noted in [5]. Similar data on the spatial distribution of temperature in the flame and in the condensed phase of the burning specimens 1, 2 and 4 are shown in Figs. 9–11. At the bottoms of the figures there are the contours of the cross sections of the extinguished specimens, as well as the temperature profiles of the fuel surface. For specimen 2, there is also the temperature profile of the lower fuel surface (dotted line). In contrast to specimens 1 and 3, on the burning surface of specimens 2 and 4 the PMMA melt boils during combustion. Extinguishing specimens 2 and 4 brought about formation of large bubbles on their surface. In the case of specimen 1, at the distance from 0 to 35 mm from the flame front the thickness of the unburnt part of the specimen did not decrease, unlike that of the other specimens. This difference seems to be related to the formation of small bubbles in

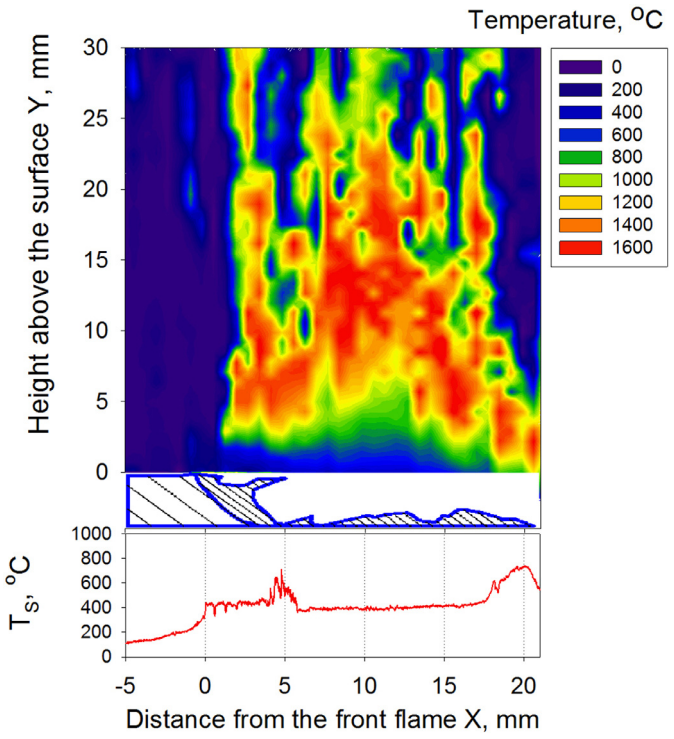

Fig. 10. The spatial distribution of temperature in the flame and in the condensed phase of the burning specimen PMMA 4. At the bottom of the figure there is the contour of the cross section of the extinguished specimen.

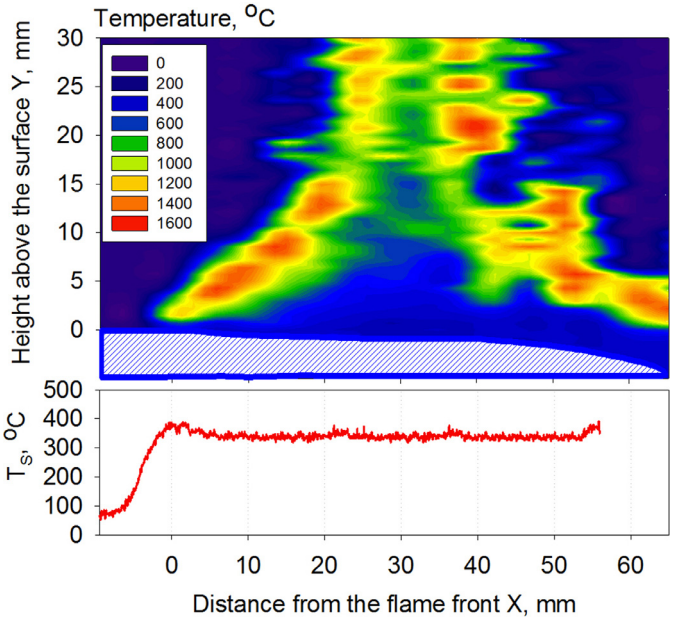

Fig. 11. The spatial distribution of temperature in the flame and in the condensed phase of the burning specimen PMMA 1. At the bottom of the figure there is the contour of the cross section of the extinguished specimen.

the mass of the fuel. The density of the unburnt part of the specimen decreased, as the distance from the flame front decreased, too, indicating the constant mass loss rate, in accordance with the measurement data. Photographs and drawings of the cross section of the extinguished specimens 2 and 4 are shown in Fig. 12. The bubbles are shown by dashed lines. Figure 13 shows the extinguished surfaces of burnt specimens, the measurements of which were used to determine the lengths of the pyrolysis zones.

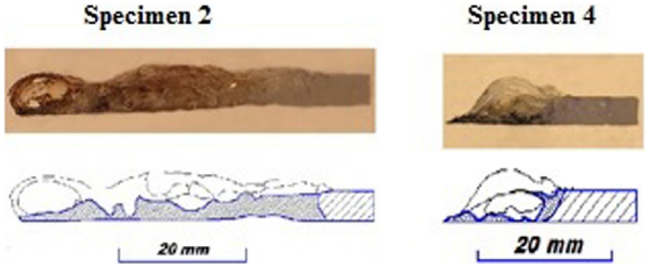

Fig. 12. Photos and drawings of the cross section of the extinguished specimens 2 and 4.

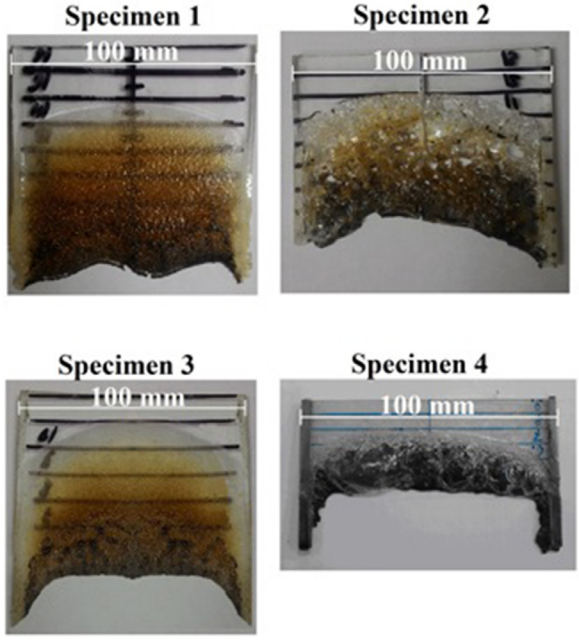

Fig. 13. The extinguished surfaces of burnt specimens 1–4 (width 100 mm).

4.3. The chemical structure of horizontally propagating flame over PMMA surface

Figures 14 and 15 show the chemical structure of horizontally propagating flame over surface of PMMA specimen 3 (width 100 mm). The main identified flame components were MMA, O_2, CO_2, H_2O, N_2, C_2H_4 (ethylene), C_3H_6 (propylene). Originally we used literature data on the composition of the PMMA pyrolysis and combustion products from [35] to identify species in the PMMA flame. In this study, using the gas chromatography method, we identified a large number of species in the PMMA and MMA flames in air counterflow, from which we chose only 12 species, the maximum concentration of which in different flame zones was higher than 0.2%: MMA, CO_2, C_3H_8, C_3H_6, O_2, N_2, CO, C_2H_4, C_2H_2, H_2O, CH_4, H_2. By measuring the mass spectra of the calibration mixtures of these species with N_2, we determined the sensitivity coefficients of the mass spectrometrometric setup. Using the intensities of the characteristic mass peaks and the sensitivity coefficients determined during calibratitons, we calculated the mole fraction of the species in the flame. Table 3 demonstrates the mass peaks, by the intensities of which species concentrations were calculated.

There are several coincident mass peaks in the mass spectra of several abovementioned species. Therefore, we measured all the mass peaks available in the mass spectra of all the 12 species in the PMMA flame. Using the results of the calibrations done, we subtracted the contributions of the species from the mass spectrum measured in the flame, beginning with the species with the

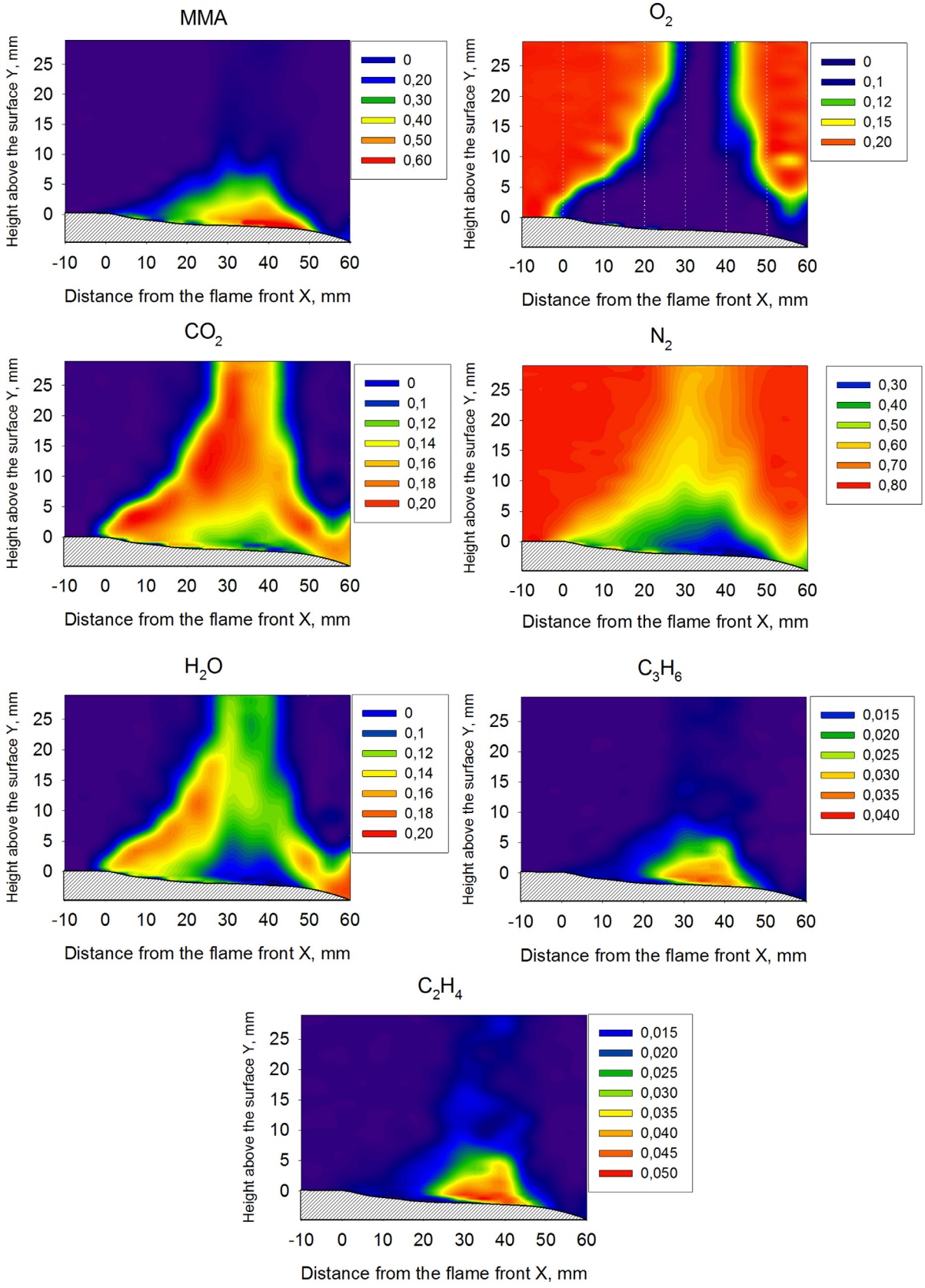

Fig. 14. Two-dimensional distribution of concentrations of major species (in mole fraction) in flame of the PMMA specimen 3, 100 mm wide.

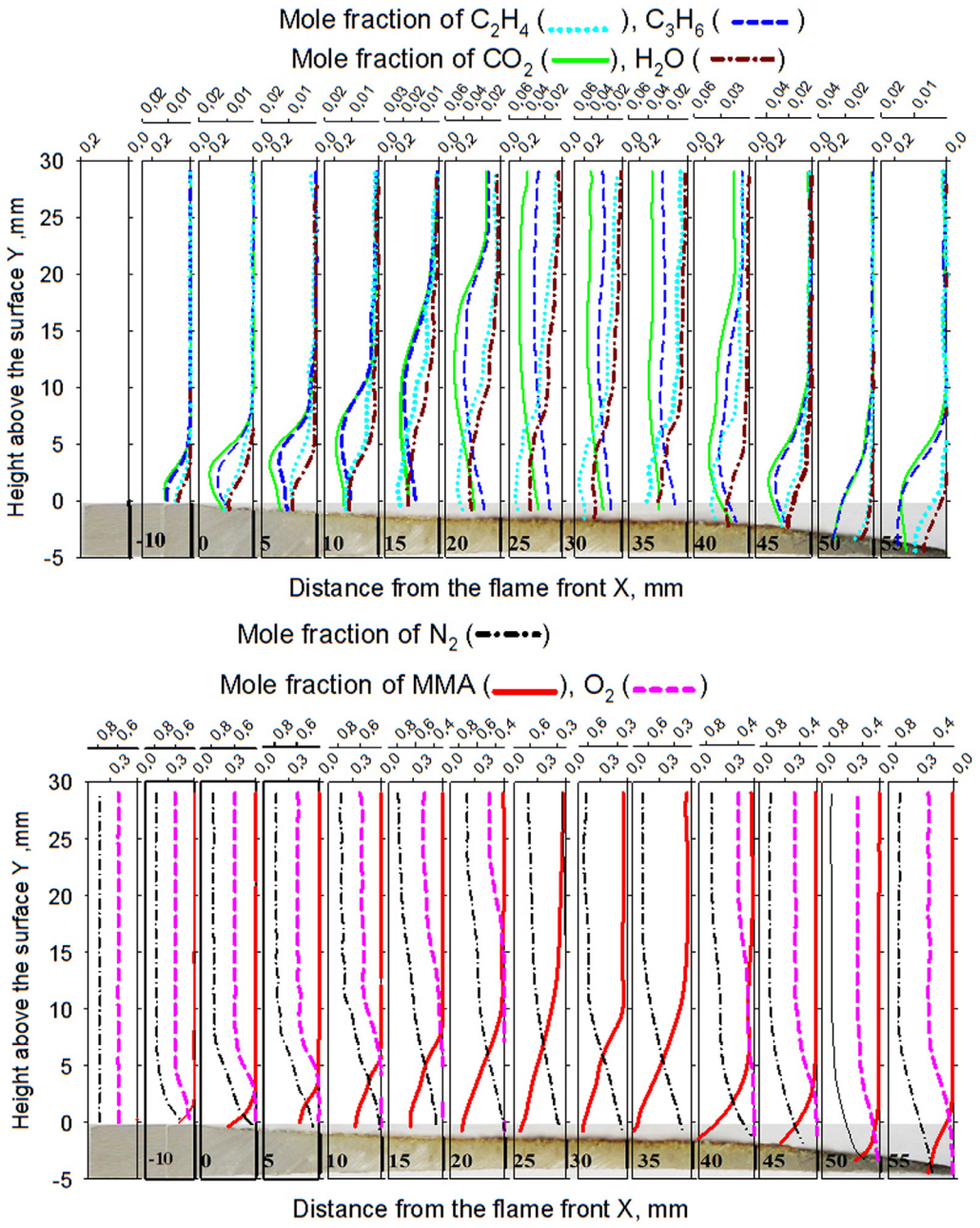

Fig. 15. Dependences of the species mole fractions on the distance from the surface (Y) of specimen 3 (100 mm wide) measured for different distances from the flame front (X).

Table 3
Species and their characteristic mass peaks (m/e), by which the species were identified and their mole fractions in the PMMA flame were calculated.

Species	MMA	CO_2	C_3H_8	C_3H_6	O_2	N_2	CO	C_2H_4	C_2H_2	H_2O	CH_4	H_2
Molecular weight	100	44	44	42	32	28	28	28	26	18	16	2
m/e	100	44	43	42	32	14	28	27	26	18	15	2

largest molecular weight (MMA) up to the lowest one (CH_4). After taking into account of the possible contributions to the characteristic mass peaks, we used their intensities to determine the mole fractions of respective species. This procedure of calculating the mole fractions of species was applied to the entire region of measurements in the flame. The results obtained showed that the maximum fraction of such species as C_3H_8, CO, C_2H_2, CH_4, and H_2 (minor species) was less than 4% in the PMMA flame, therefore, we did not consider them further and analyzed the concentration profiles of only seven major species—MMA, CO_2, C_3H_6, O_2, N_2, C_2H_4, and H_2O. Figure 14 shows variation of the species mole fraction in the gas phase over the burning specimen; the species mole fraction is shown at various heights above fuel surface versus distances X from the flame front. Figure 15 shows dependences of the species

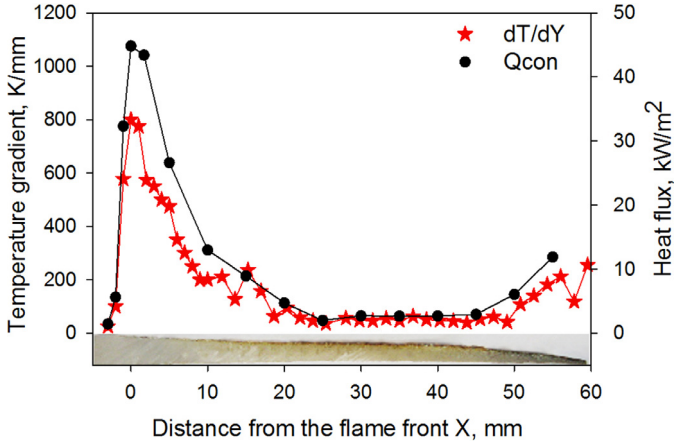

Fig. 16. Dependences of the temperature gradient and conductive heat flux to the burning surface of specimen 3 (100 mm wide) on the distance from the flame front.

mole fractions on the distance from the surface (Y) of specimen 3 measured for different distances from the flame front (X). Besides, dependences of the thickness of the unburnt part of the specimen on X are shown. (The database in the form of a table can be found in Appendix B.)

The data on the chemical flame structure have been shown to be in good agreement with those on its thermal structure. The size of the "dark zone" of the flame, in which the temperature near the polymer surface is minimal (Fig. 6), correlates well with the size of the oxygen-free zone, which is adjacent to the burning surface (Figs. 14 and 15).

4.4. Evaluation of the conductive heat fluxes from flame to polymer surface

The measured temperature profiles adjacent to the burning surface (Fig. 7) were employed to calculate the temperature gradient dT/dY (where Y is the coordinate normal to the solid fuel's surface) and to estimate the corresponding conductive heat flux Q_{con} from the flame zone to solid fuel. Distributions of the temperature gradient and the conductive heat flux along the burning surface from flame front are presented in Fig. 16 for the PMMA specimen 3. Subject to errors of temperature gradient calculation and uncertainty in determination of the thermal conductivity of gas, the accuracy of estimating the conductive heat flux stands to be at the level of 25–30%. Figure 16 shows that for the PMMA specimen 3, the maximal conductive heat flux is observed close to the flame front. Toward the end of the burning zone, where the thickness of dark flame zone decreases and oxygen concentration increases, as demonstrated above in Figs. 6, 7, 14 and 15, a certain rise of the heat flux is observed, as well as the rise of the specimen's surface temperature. In the pyrolysis zone, the average conductive heat flux on the solid fuel's surface has been shown to be 13.2 kW/m^2, which is noticeably higher than that determined in [28] for extruded PMMA produced by Nanchang Inter Industrial Co. Ltd. The average conductive heat fluxes for specimens 1, 2, and 4 are 7.6, 11.6, 8.4 kW/m^2, respectively.

The information on the cross-section shapes of the extinguished specimens (Figs. 6, 9–11) can be used for interpretation of obtained experimental data on the flame spread rate. According to the data in Table 2, specimens 1–3 show rather close values of the flame spread rate, while the flame spread rate for specimen 4 is four times less. It is noteworthy that measured pyrolysis mass rate $\dot{m}$ has actually the same value for all the tested specimens. Then, the analysis of conductive heat fluxes Q_{con} from flame to solid fuel showed its average values also to be rather close for all PMMA specimens.

The reasoned explanation of the different pyrolysis zone length of specimen 4 in comparison with the other specimens requires more detailed experimental study.

5. Conclusion

Comprehensive experimental study of flame propagating horizontally over the surface of PMMA slabs of different physical and chemical structure in still air has been performed. Following combustion characteristics have been measured: temporal dependence of the mass loss rates, the flame spread rates over the polymer surface in the steady mode, the lengths of the pyrolysis zone, and mean pyrolysis rates per unit of surface area. Also the cross-section profiles of extinguished specimens of different width and thickness have been determined. Spatial variation of temperature in the flame of all the specimens studied has been determined. Microthermocouples were used to measure the temperatures of the upper surface of the slabs versus time and the distance from the flame front. For two specimens, also the temperature profiles of the lower surface of the slabs have been measured. Spatial temperature distribution over surface of burning specimens has been determined. Dependences of flame temperature on the distance from the burning surface of the specimens, on the slab surface temperature and on the thickness of the unburnt part of the specimens at different distances from the flame front have been established. The difference in the character of combustion of the investigated specimens has been revealed. Boiling and formation of large bubbles were discovered to take place on the surface of pyrolysis and combustion of two (out of the four) specimens, in contrast to the other specimens. We were the first to measure the chemical and thermal structure of horizontally spread flame over PMMA slabs using probing mass spectrometry for a flame of condensed systems.

Following main flame species MMA, O_2, CO_2, H_2O, N_2, C_2H_4 (ethylene), C_3H_6 (propylene) have been first identified and spatial variation of their mole fractions have been measured. The measured chemical structure of the flame is in good agreement with the measured thermal flame structure. The size of the "dark zone" of the flame, in which the temperature near the polymer surface is minimal, correlates well with the size of the oxygen-free zone, which is adjacent to the burning surface. The data obtained were used to calculate the values of conductive heat flux from flame into solid fuel depending on the distance from the flame front. It has been established that the conductive heat flux is maximal in the flame front and decreases as the specimen burns out. The data obtained are valuable for understanding the mechanism of polymer combustion and may be used for developing and validating a numerical model of flame spread over PMMA surface.

Acknowledgments

This research was supported by the Russian Science Foundation (project 16-49-02017). The authors are thankful to Dr. V. Shvartsberg for useful discussion of results. The authors thank Dr. Dmitriy Parkhomenko for determining the molecular weights of studied specimens. The authors are thankful to Dr. I. Shundrina for DSC analysis.

Appendix A. Diagram of the dimensions of the metal frame and insulation board arrangement

The thermal conductivity, specific heat and specific density of the insulation board were, respectively, 0.15 W/m K, 950 J/(kg K) and 0.8 g/cm^3 (Fig. 17).

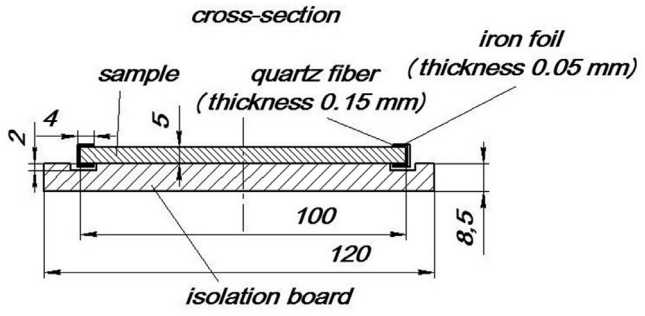

Fig. 17. Diagram of the dimensions of the metal frame and insulation board arrangement.

Appendix B. Supplementary material

Supplementary data in the form of a table including temperature distribution in the gas and solid phase, two-dimensional distribution of concentrations profiles of major species (in mole fraction) in flame of the PMMA specimen 3 can be accessed on the publisher's website.

Supplementary material associated with this article can be found, in the online version, at doi:10.1016/j.combustflame.2017.10.008.

References

[1] A.C. Fernandez-Pello, F.A. Williams, Laminar flame spread over PMMA surfaces, Symp. (Int.) Combust. 15 (1975) 217–231.
[2] AC. Fernandez-Pello, F.A. Williams, A theory of laminar flame spread over flat surfaces of solid combustibles, Combust. Flame 28 (1977) 251–277.
[3] A.C. Fernández-Pello, F.A. Williams, Experimental Techniques in the study of laminar flame spread over solid combustibles, Combust. Sci. Technol. 14 (4) (1976) 155–167.
[4] M. Sibulkin, A. Hansen, Experimental study of flame spreading over a horizontal fuel surface, Combust. Sci. Technol. 10 (1) (1975) 85–92.
[5] S.R. Ray, A.C. Fernandez-Pello, I.A. Glassman, A study of the heat transfer mechanisms in horizontal flame propagation, J. Heat Transfer 102 (2) (1980) 357–363.
[6] M. Sibulkin, J. Kim, J.V. Creeden, The dependence of flame propagation on surface heat transfer. I. Downward burning, Combust. Sci. Technol. 14 (1976) 43–56.
[7] A.E. Frey, J.S. T'ien, A theory of flame spread over a solid fuel including finite-rate chemical kinetics, Combust. Flame 36 (1979) 263–289.
[8] T. Hirano, S.E. Noreikis, T.E. Waterman, Measured velocity and temperature profiles near flames spreading over a thin combustible solid, Combust. Flame 23 (1974) 83–96.
[9] I.S. Wichman, Theory of opposed-flow flame spread, Prog. Energy Combust. Sci. 18 (1992) 553–593.
[10] M.A. Delichatsios, Exact solution for the rate of creeping flame spread over thermally thin materials, Combust. Sci. Technol. 44 (1986) 257–267.
[11] I.T. Leventon, J. Li, S.I. Stoliarov, A flame spread simulation based on a comprehensive solid pyrolysis model coupled with a detailed empirical flame structure representation, Combust. Flame 162 (2015) 3884–3895.
[12] K.K. Wu, W.F. Fan, C.H. Chen, T.M. Liou, I.J. Pan, Downward flame spread over a thick PMMA slab in an opposed flow environment: experiment and modeling, Combust. Flame 132 (2003) 697–707.
[13] S. Bhattacharjee, M.D. King, C. Paolini, Structure of downward spreading flames: a comparison of numerical simulation, experimental results and a simplified parabolic theory, Combust. Theor. Model. 8 (2004) 23–39.
[14] C.P. Mao, H. Kodama, A.C. Fernandez-Pello, Convective structure of a diffusion flame over a flat combustible surface, Combust. Flame 57 (1984) 209–236.
[15] C.H. Chen, A numerical study of flame spread and blowoff over a thermally-thin solid fuel in an opposed air flow, Combust. Sci. Technol. 69 (1990) 63–83.
[16] A. Kumar, H.Y. Shih, J.S. T'ien, A comparison of extinction limits and spreading rates in opposed and concurrent spreading flames over thin solids, Combust. Flame 132 (2003) 667–677.
[17] C. Di Blasi, Modeling and simulation of combustion processes for charring and non-charring solid fuels, Prog. Energy Combust. Sci. 19 (1993) 71–104.
[18] A.C. Fernandez-Pello, S.R. Ray, I.A. Glassman, Flame spread in an opposed forced flow: the effect of ambient oxygen concentration, Symp. (Int.) Combust. 18 (1981) 579–589.
[19] A.C. Fernandez-Pello, T. Hirano, Controlling mechanisms of flame spread, Fire Sci. Technol. 1 (1982) 17–54.
[20] A. Ito, T. Kashiwagi, Characterization of flame spread over PMMA using holographic interferometry sample orientation effects, Combust. Flame 71 (1988) 189–204.
[21] A. Ito, T. Kashiwagi, Temperature measurements in PMMA during downward flame spread in air using holographic interferometry, Symp. (Int.) Combust. 21 (1987) 65–74.
[22] N. Iqbal, J. Quintiere, Flame heat fluxes in PMMA pool fires, J. Fire Prot. Eng. 6 (4) (1994) 153–162.
[23] Y. Pizzo, C. Lallemand, A. Kacema, A Kaiss, J. Gerardin, Z. Aceme, P. Boulet, B. Porterie, Steady and transient pyrolysis of thick clear PMMA slabs, Combust. Flame 162 (2015) 226–236.
[24] I.T. Leventon, S.I. Stoliarov, Evolution of flame to surface heat flux during upward flame spread on poly(methyl methacrylate), Proc. Combust. Inst. 34 (2013) 2523–2530.
[25] Y. Pizzo, J.L. Consalvi, P. Querre, M. Coutin, L. Audouin, B. Porterie, Experimental observations on the steady-state burning rate of a vertically oriented PMMA slab, Combust. Flame 152 (2008) 451–460.
[26] J.G. Quintiere, Fundamentals in fire phenomenon, John Wiley & Sons Ltd, 2006.
[27] L. Jiang, H.H. Xiao, Y. Zhou, W. An, W. Yan, J. He, J. Sun, Theoretical and experimental study of width effects on horizontal flame spread over extruded and expanded polystyrene foam surfaces, J. Fire Sci. 32 (3) (2014) 193–209.
[28] L. Jiang, C.H. Miller, M.J. Gollner, J.-H. Sun, Sample width and thickness effects on horizontal flame spread over a thin PMMA surface, Proc. Combust. Inst. 36 (2017) 2987–2994.
[29] S.I. Stoliarov, R.N. Walters, Determination of the heats of gasification of polymers using differential scanning calorimetry, Polym. Degrad. Stab. 93 (2008) 422–427.
[30] W.E. Kaskan, The dependance of flame temperature on mass burning velocity, Symp. (Int.) Combust. 6 (1957) 134.
[31] A.V. Singh, M.J. Gollner, Estimation of local mass burning rates for steady laminar boundary layer diffusion flames, Proc. Combust. Inst. 35 (3) (2015) 2527–2534.
[32] A.V. Singh, M.J. Gollner, A methodology for estimation of local heat fluxes in steady laminar boundary layer diffusion flames, Combust. Flame 162 (5) (2015) 2214–2230.
[33] S. Bhattacharjee, M. Bundy, C. Paolini, G. Patel, W. Tran, A novel apparatus for flame spread study, Proc. Combust. Inst. 34 (2013) 2513–2521.
[34] O.P. Korobeinichev, L.V. Kuibida, A.A. Paletsky, A.G. Shmakov, Development and application of molecular beam mass-spectrometry to the study of ADN combustion chemistry, J. Propul. Power 14 (6) (1998) 991–1000.
[35] K. Seshadri, F.A. Williams, Structure and extinction of counterflow diffusion poly(methy1 methacrylate) and its liquid monomer, both burning in nitrogen–air mixtures, J. Polym. Sci. Part A: Polym. Chem. 16 (1978) 1755–1778.